Figure 5. Cyclic voltammogram of BPPI layer on TiO$_2$.

redox couple multilayer. Although UV spectra, ellipsometric measurements, and cyclic voltammogram suggest that the Zr-BPPI films grow uniformly, the atomic images of multilayer films are needed to confirm the uniformity of films. Therefore, the AFM measurement of Zr-BPPI films is being carried out to study film uniformity and growth on a microscopic level.

In summary, it is shown that the layer thickness measured by ellipsometry linearly increases as a function of the number of layer deposited and UV-vis spectroscopic results of the deposition process are consistent with those of ellipsometric measurements. The average thickness of the film derived by ellipsometry was observed about 15.8 Å. Also, according to cyclic voltamogram, the quasi-reversible peak currents are systematically increased as the number of layer increases. These results indicate that the same amount of BPPI layer is placed on the substrate after each deposition cycle.

References

1. Dines, M. B.; Griffith, P. C. *Inorg. Chem.* **1983**, *22*, 567.

2. Zeppenfeld, A. C.; Fiddler, S. L.; Ham, W. K.; Klopfenstein, B. J.; Page, C. J. *J. Am. Chem. Soc.* **1994**, *116*, 9158.
3. (a) Lee, H.; Kepley, L. J.; Hong, H. G.; Mallouk, T. E. *J. Am. Chem. Soc.* **1988**, *110*, 618. (b) Akhter, S.; Lee, H.; Hong, H. G.; Mallouk, T. E.; White, J. M. J. *J. Vac. Sci. Technol.* **1989**, *7*, 1608.
4. Vermeulen, L. A.; Snover, J. L.; Sapochak, L. S.; Thomson, M. E. *J. Am. Chem. Soc.* **1993**, *115*, 11767.
5. Law, K. Y. *Chem. Rev.* **1993**, *93*, 449.
6. Heribert, Q.; Yves, G.; Klaus, M. *Chem. Mater.* **1997**, *9*, 495.
7. Halls, J. J. M.; Friend, R. H. *Synthetic Metals.* **1997**, *85*, 1307.
8. Langhals, H. *Chem. Ber.* **1985**, *118*, 4641.
9. (a) Putvinski, T. M.; Schilling, M. L.; Katz, H. E. *Langmuir.* **1990**, *6*, 1567. (b) Katz, H. E.; Wilson, W. L.; Scheller, G. *J. Am. Chem. Soc.* **1994**, *116*, 6636. (c) Katz, H. E.; Scheller, G.; Putvinski, T. M.; Schilling, M. L.; Wilson, W. L.; Chidsey, C. E. D. *Science.* **1991**, *254*, 1485.
10. Snover, J. L.; Byrd, H.; Suponeva, E. P.; Vicenzi, E.; Thomson, M. E. *Chem. Mater.* **1996**, *8*, 1490.
11. Nanoporous TiO$_2$ film electrode was prepared using Degussa P25 TiO$_2$ by the method of Graetzel et al's[12]. The thickness of the TiO$_2$ film is about 4 μm estimated from SEM picture. The geometric area of the electrode is 1.5 cm^2. However the actual surface area of the TiO$_2$ electrode is about 1000 times higher than that considering nanoporous nature. The cyclic voltammograms were measured in three cell electrode system with Pt counter and SCE reference electrode. The electrolyte solution was 0.1 M KCl and the scan rate was 25 mV/sec. The detail electrochemical studies of these multilayers on the TiO$_2$ electrode will be presented in the other paper.
12. Nazeerudin, M. K.; Rodicio, I. R.; Baker, H.; Liska, P.; Vlachopoulos, N.; Grizel, M. *J. Am. Chem. Soc.* **1993**, *115*, 6382.

Kinetic Analysis of Inactivation of the cdc25 Phosphatase by Menadione

Seung Wook Ham*, **Ji Sang Yoo, Junguk Park, and Hyeongjin Cho†**

*Department of Chemistry, Chung-Ang University, Seoul 156-756, Korea*
†Department of Chemistry, Inha University, Inchon 402-751, Korea
Received September 26, 1997

Cdc25 phosphatases catalyze tyrosine-15 dephosphorylation of the p34^{cdc2}, catalytic subunit of the M phase-Promoting Factor (MPF);[1,2] this leads to the G2/M transition of the cell cycle in all organisms.[3,4] These enzymes play an important role in the regulation of cell division cycle and present a promising target for the design of potential chemotherapeu-

tic agents in the field of antitumor treatment.[5~7]

Since it has been reported that menadione induced alterations in the phosphorylation status and the activity of protein tyrosine phosphatase,[8] and menadione shares a enone structure with some mechanism-based inhibitors of phosphatases that have been previously reported,[9,10] we have re

30 *Bull. Korean Chem. Soc.* **1998**, Vol. 19, No. 1
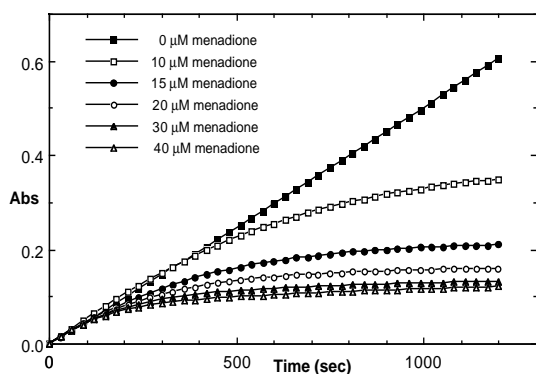
Communications to the Editor
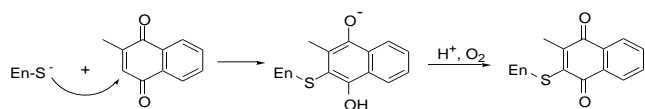
Scheme 1.

cently investigated the effects of menadione on the activity of cdc25A phosphatase. We suggested that cdc25A phosphatase was inactivated by menadione and that the loss of enzyme activity was due to the modification of the active site as illustrated in Scheme 1.[11] We describe here that this novel class of enzyme inhibitor efficiently inactivate the cdc25A phosphatase.

To determine the efficiency of enzyme inactivation by menadione, we continuously monitored at 410 nm and 37.0 ± 0.1 °C by a JASCO UV/Vis spectrophotometer equipped with a JASCO peltier type thermostatic cell holder. The GST-cdc25A phosophatase instead of cdc25A phosophatase was used for kinetic analysis because a screening system for inhibitors of this enzyme has been well described.[5] Thus, purified GST-cdc25A phosphatase (0.2 mg/mL) was incubated with the chromogenic substrate, 40 mM *p*-nitrophenyl phosphate in 20 mM Tris (pH 8.0), 1 mM EDTA, and 0.2 mM DTT. Figure 1 depicts the time course of the reaction in the absence of or presence of increasing concentration of menadione. In the absence of menadione, a straight line is obtained from the plot of absorbance (yield of p-nitrophenolate) at 410 nm versus time. In the presence of menadione p-nitrophenolate formation decreases with increasing concentration of menadione. This result indicates the menadione inactivates the GST-cdc25A phosphatase. Like cdc25A phosphatase, the activity of inactivated enzyme with menadione did not return, even after exhaustive dialysis, suggesting an irreversible inactivation process. Moreover, moderate protection from inhibition in the presence of the competitive reversible inhibitor, arsenate, shows that menadione reacts with the active site of the enzyme (data not shown).[10]

From these data, the rate of enzyme inactivation by menadione could be evaluated by determining the K_i and k_{inact} using the method of Kitz and Wilson.[11]

$$En_{act} + I \underset{K_i}{\rightleftarrows} En \cdot I \xrightarrow{k_{inact}} En_{inact}$$

The solution of the equations is

$$\ln[E]_r/[E]_o = -k_{inact}t/(1 + K_i/[I])$$

Let

$$k_{app} = k_{inact}/(1 + K_i/[I])$$
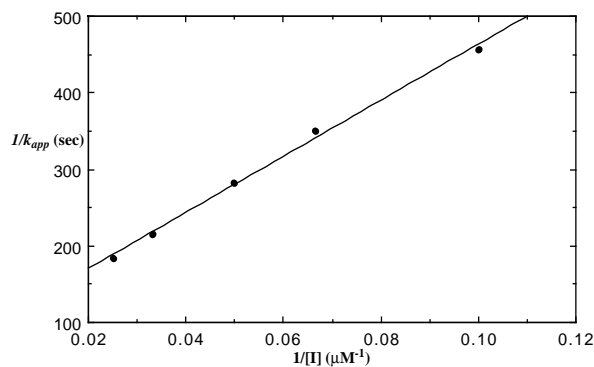
Then

$$1/k_{app} = (K_i/k_{inact})/[I] + 1/k_{inact} \qquad (1)$$

Since the plot of p-nitrophenolate formation versus GST-cdc25A concentration is linear and the rate is directly proportional to the concentration of active enzyme at large amount of substrate, the fraction of enzyme activity remaining ($[E]_r/[E]_o$) could be substituted by the ratio of instantaneous rate at a particular time to instantaneous rate at $t = 0$. The rate at $t = 0$ is the slope of the straight line in the absence of menadione in Figure 1. Therefore, $[E]_r/[E]_o$ was determined by the ratio of the differentiation of the curves with variable concentrations of inhibitor to the slope of the control (without menadione). We obtained the plot of $\ln([E]_r/[E]_o)$ versus time which is shown in Figure 2. The values of an apparent rate constant k_{app} for the reaction were then determined from the slope of the straight lines in Figure 2. Finally, these were plotted as a reciprocal versus 1/[I]. The five data points (•) in Figure 3 appears to lie on a with a slope of 3700 and inter-
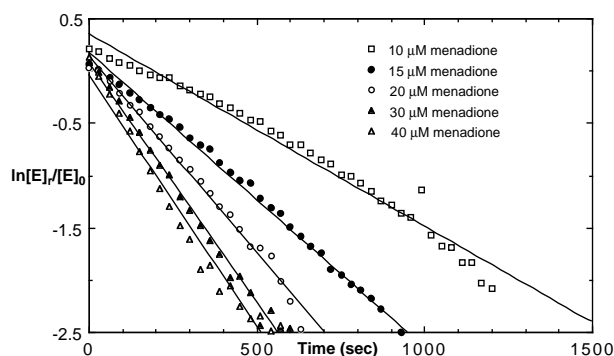
Figure 2. Time dependence and concentration dependence of the inactivation of GST-cdc25A phosphatase with menadione.

Figure 1. Time course of the reaction of cdc25A phosphatase in the absence of or presence of menadione (10-40 mM). Freshly prepared solutions of menadione in isopropyl alcohol were added in amounts up to 0.002 mL per 1 mL of reaction mixture. Similar amounts up to isopropyl alcohol alone had no effect on the reaction studied.

Figure 3. The dependence of k_{app} upon the concentration of menadione plotted as double reciprocals in accordance with equation 1.
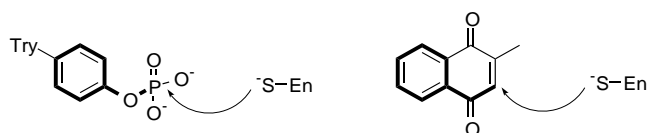
Figure 4. Structural similarity of phosphotyrosine and menadione.

cept on the vertical axis is 95. From the data plotted in accordance with equation 1, the values found for the dissociation constant K_i and the inactivation rate constant k_{inact} were $38 \pm 4 \times 10^{-6}$ M and $1.05 \pm 0.08 \times 10^{-2}$ sec^{-1}, respectively. These values compare very favorably with those for mechanism-based inhibitors of phosphatases.[9,10]

As shown in Figure 4, menadione shares critical structural features with phosphotyrosine. Therefore, menadione might have the favorable dissociation constant. For example, incubation of cdc25 phosphatase with 1,4-benzoquinone did not show inhibition, suggesting that the aromatic ring of inactivator is necessary for its action.

In conclusion, the active site of cdc25A phosphatase could be irreversibly inactivated by menadione. We have also been able to provide data, K_i and k_{inact}, that show the efficiency of inactivation. Based on these data, modifying the inactivator is matter of future interest.

References

1. Gould, K. L.; Moreno, S.; Tonks, N. K.; Nurse, P. *Science* **1990**, *250*, 1573.
2. Nurse, P. *Nature* **1990**, *344*, 503.
3. Russell, P.; Moreno, S.; Reed, S. I. *Cell* **1989**, *57*, 295.
4. Edger, B. A.; O'Farrell, P. H. *Cell* **1990**, *57*, 469.
5. Baratte, B.; Meijer, L.; Galaktionov, K.; Beach, D. *Anticancer Res.* **1992**, *12*, 873.
6. Galaktionov, K.; Lee, A. K.; Eckstein, J.; Draetta, G., Meckler, J.; Loda, M.; Beach, D. *Science* **1995**, *269*, 1575.
7. Gunasekera, S. P.; McCarthy, P. J.; Kelly-Borges, M.; Lobkovsky, E.; Claydy, J. *J. Am. Chem. Soc.* **1996**, *118*, 8759.
8. Juan, C.-C.; Wu, F. Y.-H. *Biochem. Biophys. Res. Commun.* **1993**, *190*, 907.
9. Myers, J. M.; WidlanskiI, T. S. *Science* **1993**, *262*, 1451.
10. Myers, J. M.; Cohen, J. D.; WidlanskiI, T. S. *J. Am. Chem. Soc.* **1995**, *117*, 11049.
11. Ham, S. W.; Park, H. J.; Lim, D. H. *Bioorg. Chem.* **1997**, *25*, 33.
12. Kitz, R.; Wison, I. B. *J. Biol. Chem.* **1962**, *237*, 3245.

Affirmation of a general base of *Hafnia alvei* Aspartase by Organic Solvent Perturbation Method

Moon-Young Yoon[*] and Cheon-Gyu Cho

Department of Chemistry, Hanyang University, Seoul 133-791, Korea
Received October 7, 1997

Aspartase (L-aspartate ammonia-lyase, EC4.3.1.1) catalyzes the reversible conversion of L-aspartate to fumarate and ammonia.[1] The enzyme is specific for aspartate and fumarate, but NH_2OH can be substituted for ammonia as a substrate.[2,3] A variety of divalent metal ions, such as Mg^{2+}, Mn^{2+}, Zn^{2+} and Co^{2+} activate the reaction.[4] Initial velocity studies obtained for the enzyme from Hafnia alvei are consistent with a rapid equilibrium kinetic mechanism in which Mg^{2+} binds prior to aspartate, but with a random release of Mg^{2+}, NH_4^+, or fumarate.[5]

An acid-base chemical mechanism for *Hafnia alvei* aspartase has been proposed using pH studies and deuterium wash-in[6,7] (scheme 1). Data are consistent with a proton which is abstracted from C-3 of the monoanionic form of aspartate by an enzyme general base with a pK of 6.3-6.6 in the absence and presence of Mg^{2+}. The resulting carbanion is presumably stabilized by delocalization of electrons into the β-carboxyl with the assistance of a protonated enzyme group in the vicinity of the β-carboxyl. Ammonia is then expelled with the assistance of a general acid group that traps an initially expelled NH_3 as the final NH_4^+ product. The pK for the general acid is about 7 in the absence of Mg^{2+}, but is increased by about a pH unit in the presence of Mg^{2+}. Since the same pK values are observed in the p$Ki_{succinate}$ and V/K pH profile, both enzyme groups must be in their optinum protonation state for efficient binding of reactant in the presence of Mg^{2+}. At the end of a catalytic cycle, both the general base and general acid groups are in a protonation state opposite that in which they started when aspartate was bound. When the aspartase reaction is run in D_2O to greater than 50% completion no deuterium is found in the remaining aspartate, indicating that the site is inaccessible to solvent during the catalytic cycle.[7]

Construction of a reaction mechanism for an enzyme requires a knowledge of its amino acid or other residues involved in the catalytic process. One method for identifying the charge types at the active site of an enzyme is based on the use of organic solvents perturbation.[8] The solvent pertur